

# Prediction of Failure Behaviors in Polymers Under Multiaxial Stress State

Shinya Hayashi

JSOL Corporation

2-18-25 Marunouchi, Naka-ku, Nagoya

Aichi, 460-0002, Japan

## Abstract

*Polymers are used in an increasing number of automobile parts to improve occupant and pedestrian safety as well as reduce weight and cost. Under impact, these parts are designed to effectively absorb energy through large deformation and failure. Failure phenomena are very important to predict because structural strength is drastically changed or lost after failure occurs.*

*In this study, puncture tests for polypropylene sheets were performed at various impact velocities and frictions, and failure locations and timings in the sheets were investigated. Puncture tests generate a multiple stress state in the sheets and this heavily influences the failure behavior of the sheet material. CAE crash simulations using LS-DYNA were conducted to successfully predict deformation and failure behavior under a multiaxial stress state.*

## Introduction

The prediction of failure behavior in polymer materials is very important and has been investigated with numerical crash simulation for a long time [1-6]. Material models for polymers have been implemented in LS-DYNA and also some LS-DYNA users have been developed user material models with their own constitutive equations for polymers. Such material models have shown good performance in predicting the deformation behaviors of polymers. However, in the case of complicated deformation modes there are still some failure phenomena that are not well predicted.

In material tests of polymers, uniaxial tension and sometimes compression tests are generally executed and material models validated using dynamic uniaxial tension or 3-point bending tests. However, in a realistic impact situation, a biaxial as well as uniaxial stress state is generated in the component. It is known from literature that biaxial tension stress state can be assessed by puncture tests. In this study, deformation and failure behaviors of polymer sheets in puncture tests have been investigated.

All calculations in this study were executed using \*MAT\_SAMP-1 (Semi-Analytical Model for Polymers) and \*MAT\_ADD\_EROSION implemented in LS-DYNA 971 R6.0.0 [7]. No user material subroutines were investigated. \*MAT\_SAMP-1 can have an isotropic C-1 smooth yield surface taking biaxial tension property into account [1]. \*MAT\_ADD\_EROSION can treat failure plastic strain dependent on the deformation mode (stress triaxiality) in its GISSMO functions [8].

Finally, correlation studies of the failure behaviors were assessed. Where problems and limitations of predictions were encountered, new features for adding to LS-DYNA are proposed.

Pre- and post-processing of the LS-DYNA simulations in this study were done using PRIMER and D3PLOT developed by Ove Arup & Partners.

## Material Tests for Polypropylene

Polypropylene is one of the most widely used polymer materials and made into various commercial mass products. In this study, a non-reinforced polypropylene material was selected. At first, flat sheets of 2mm thickness were produced by an injection molding process and then the various material tests (except for biaxial tension) were carried out to develop the input for \*MAT\_SAMP-1. The injection molding process created an orthogonal material property in the plate: the stiffness in the flow direction was about 10% higher than the cross flow direction. In our tensile and compression tests all specimens were cut out in the flow direction.

- 1) Static and dynamic uniaxial tension tests (0.01/s, 0.1/s, 1.0/s, 10/s, 100/s)
- 2) Static uniaxial compression test
- 3) Static shear test
- 4) Plastic Poisson's Ratio test

\*MAT\_SAMP-1 can have an isotropic C-1 smooth yield surface created from various material tests to simulate realistic polymer deformation [1]. However in this study, biaxial tension test results were not available because it was difficult to create precise cross-shape specimens of the polymer material and the measurement of a pure biaxial tension property was not successful. Therefore, instead of biaxial tension, a puncture test was conducted. Details of the puncture test are discussed in later sections.

Figure 1 shows the uniaxial tensile material properties of this polypropylene under static and dynamic loading. There is no failure in the static case (below 0.01/s), the material was very ductile. Under dynamic loading (over 0.1/s), material failure occurred at strains from 15% to 60%, becoming more brittle at higher strain rates.

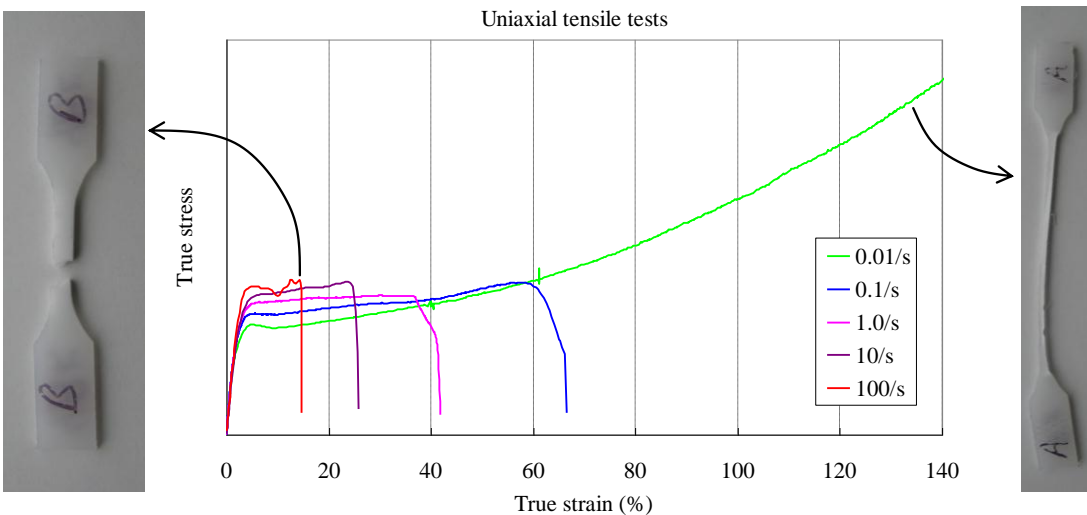


Figure 1: Uniaxial tension properties measured in static and dynamic tests.

## Puncture tests

A puncture test is a kind of falling weight impact test to measure impact strength and energy absorption. This test is defined by the international standard ISO 6603-2 [9]. A hemisphere shape striker hits and penetrates a specimen sheet. Figure 2 shows the puncture test machine used in this study and shapes and sizes of a striker and clamping jigs. The striker in this puncture machine can be kept at constant velocity by a hydraulic system. A 2mm thickness flat plate was used as specimen sheet.

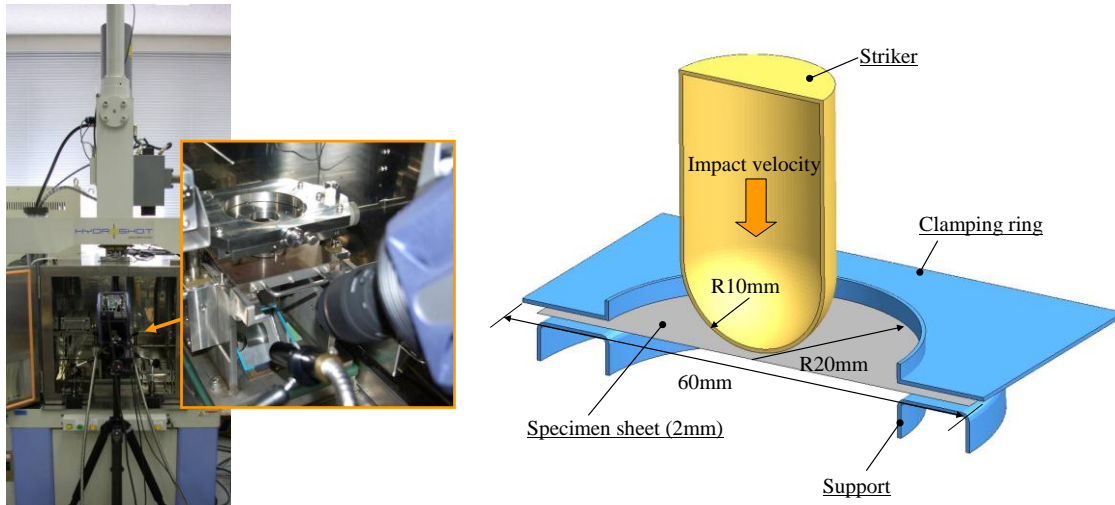


Figure 2: Puncture test machine, striker and clamping jigs of ISO6603-2.





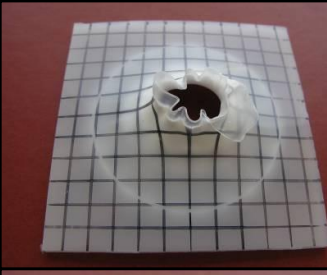
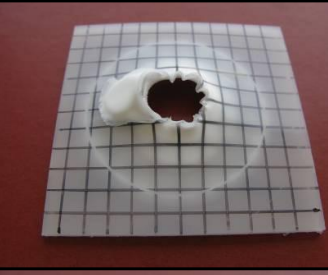

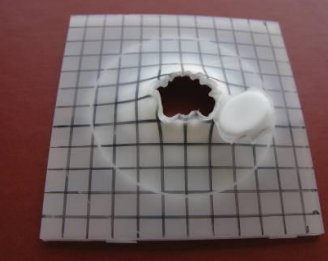
Table 1 shows the eight puncture tests carried out in this study, which had the combination of four impact velocities at both low and high friction between the striker and the sheet. Each test was executed 2 times to determine variability and errors. The impact velocities were decided from automobile regulations or assessment tests; 5km/h represents low speed impact (IIHS Low-Speed Crash Test, FMVSS Part 581), 24km/h for interior head impact (FMVSS 201, ECE-R21) and 40 km/h for pedestrian lower leg impact (EuroNCAP). The friction condition was determined by adding lubricant to the striker head: by coating the striker with lubricant the friction coefficient was dropped to roughly zero. By ensuring zero lubricant on the striker the friction coefficient was raised to a value of roughly between 0.3 and 0.4.

Table 1: Puncture tests

Test ID	Impact velocity (km/h)	Friction (Lubricant)
SL	Static (0.001)	low (coated)
SH		High (not coated)
5L	5.0	low (coated)
5H		High (not coated)
24L	24	low (coated)
24H		High (not coated)
40L	40	low (coated)
40H		High (not coated)

Table 2 shows pictures of deformed sheets after the tests. Two types of rupture mode are apparent, generated by the different friction conditions. This is not unknown phenomenon, as documented in ISO 6603-2 [9]. Figure 3 shows a simplified diagram of the two modes known as petaling and circumferential failure modes [10].

Table 2: Sheet deformation modes of each test

Friction Velocity	Low	High
Static		
5 km/h		
24 km/h		
40 km/h		

Petaling failure

Circumferential failure

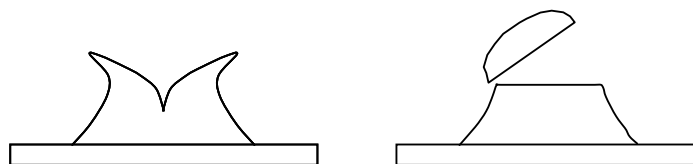


Figure 3: Two types of failure mode

Figure 4 shows the striker force-displacement curves from the low and high friction tests. Peak forces in the high friction tests were higher than in the low friction tests. This increase of peak force at higher friction is also documented in ISO6603-2 [9].

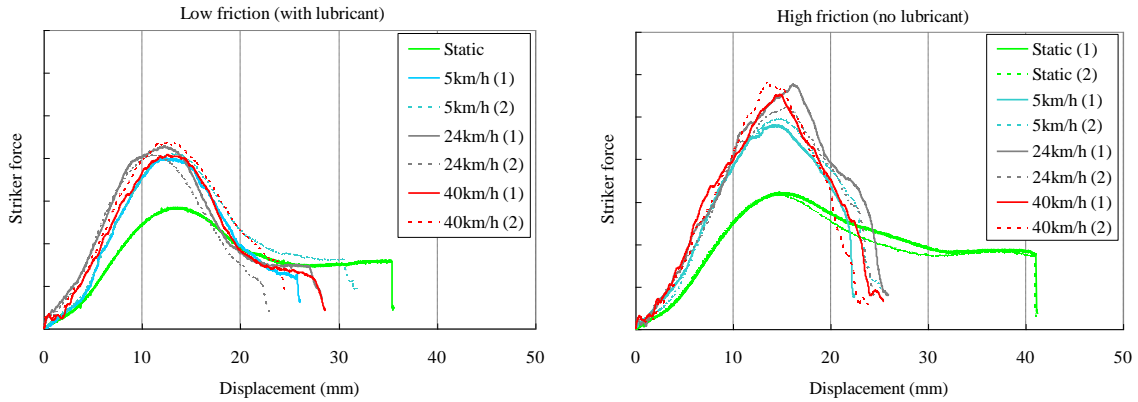


Figure 4: Striker force vs. displacement curves in low and high friction tests

In the four tests of 24L/H and 40L/H, 5mm pitch grid lines were drawn on the sheets and the deformation behavior recorded by high speed video camera. The changing shape of the 5mm pitch grid lines provided a rough indication of strain distribution and deformation mode. Figure 5a and 5b are pictures at striker displacement 18mm and 28mm from tests 40L and 40H. These pictures allow observation of the exact timing and location of initial rupture.

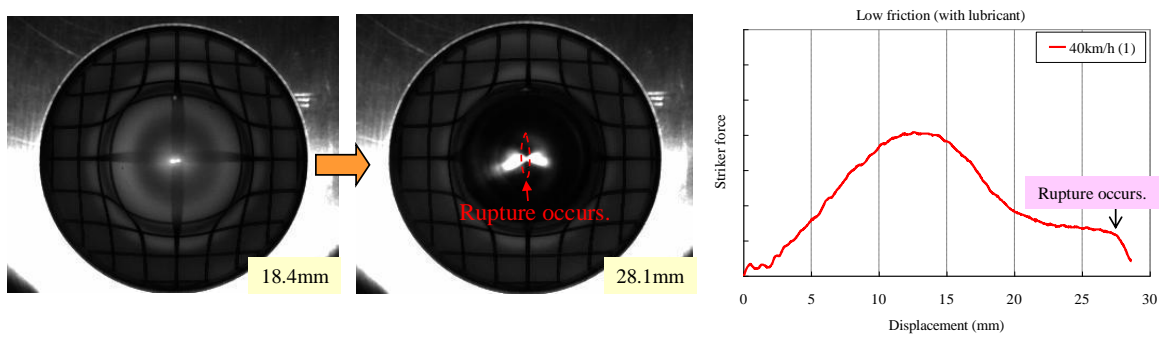


Figure 5a: Initial rupture under low friction at impact velocity 40km/h (40L)

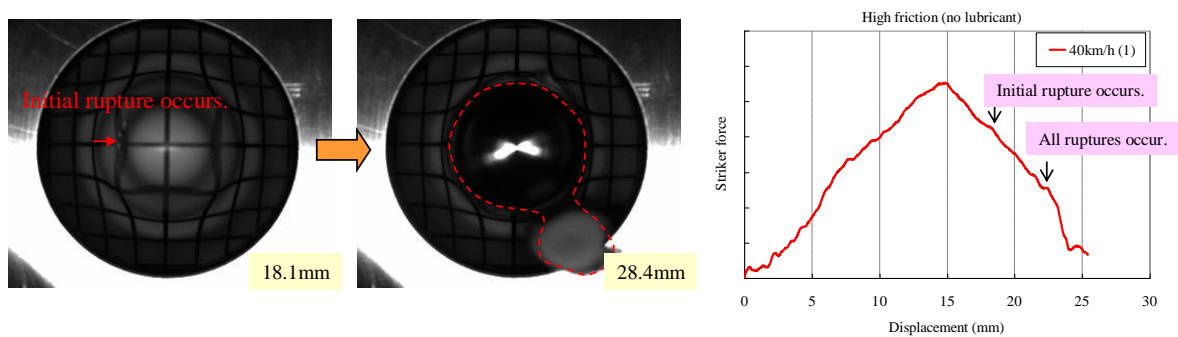


Figure 5b: Initial rupture under high friction at impact velocity 40km/h (40H)

### Development of material model for puncture test simulation

The material sheet model used in the LS-DYNA puncture simulation was meshed as shell elements of 1mm length and 2mm thickness, using \*MAT\_SAMP-1. Figure 2 shows the shape of striker and clamping jigs created according to ISO603-2 test specifications and they were modelled using a rigid material. Puncture simulations were performed using LS-DYNA 971 R6.0.0.

In an initial run, \*MAT\_SAMP-1 was input using data measured from static and dynamic uniaxial tension tests, also uniaxial compression, shear and plastic Poisson’s Ratio, but did not include biaxial tension data. A puncture simulation at impact velocity 40km/h was calculated with no friction between the striker and the sheet. Figure 6 shows striker force-displacement curve compared with the test result. Stiffness of LS-DYNA result was larger than the test results and no peak force appeared in the LS-DYNA result.

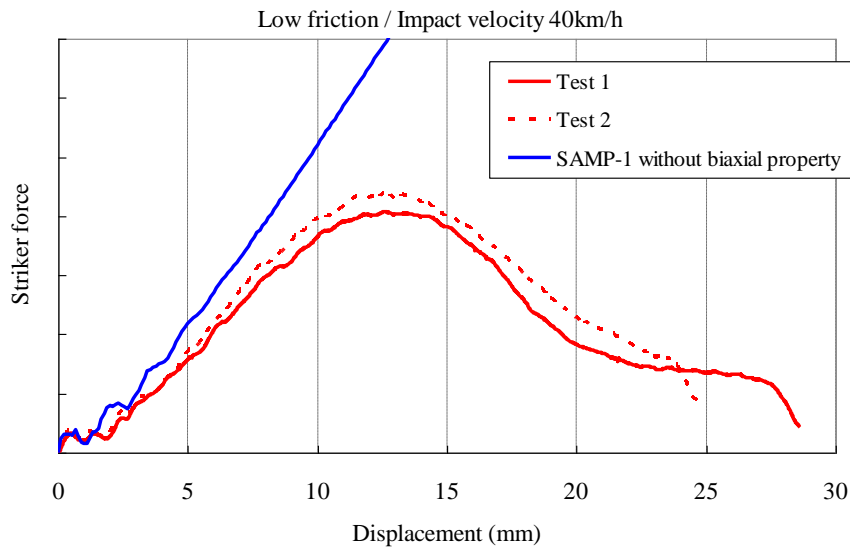


Figure 6: Striker force vs. displacement results (initial run)

Figure 7 shows stress triaxiality distribution in the sheet during the simulation. The sheet deformed under a stress triaxiality of 2/3, which means biaxial tension deformation. As expected, the sheet response measured in puncture tests is dominated by its biaxial tensile properties.

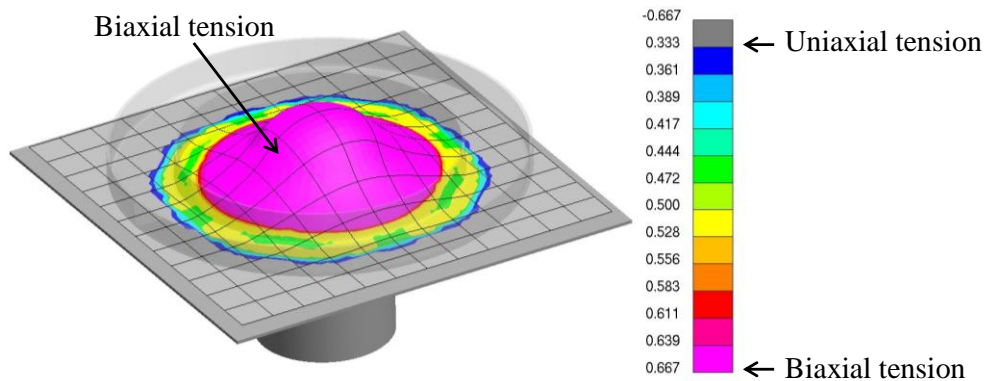


Figure 7: Stress triaxiality distribution (deformation mode) in sheet during puncture test

To make the stiffness of the LS-DYNA prediction closer to test, a static uniaxial tensile curve scaled by 0.7 was input for the biaxial tensile property in \*MAT\_SAMP-1. Figure 8 shows how the initial slope of predicted striker force was brought closer to test by adding the biaxial tension property. The isotropic C-1 smooth yield surface of \*MAT\_SAMP-1 was improved by adding the biaxial tension property.

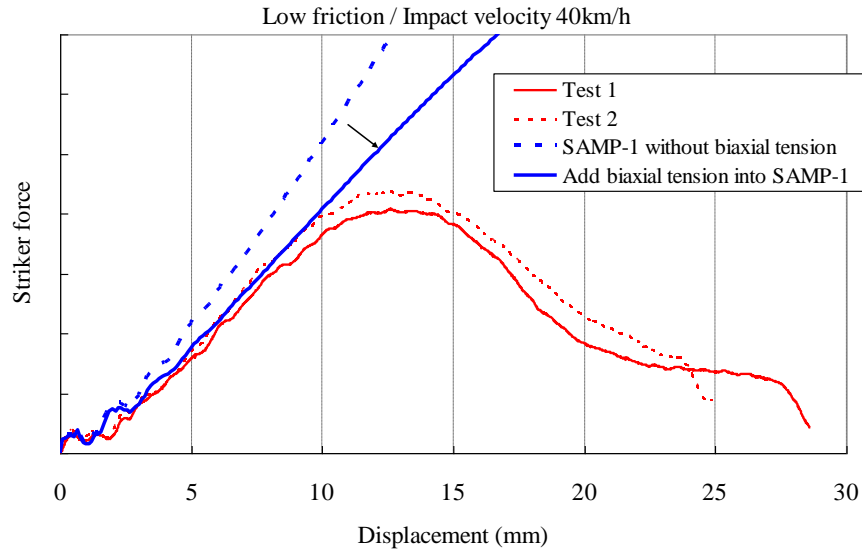


Figure 8: Striker force vs. displacement result tuned with biaxial tension property

However, the model did not predict the peak then drop in striker force that occurred in test. It was therefore considered that some form of damage phenomenon occurred under biaxial tension deformation. Damage property can be input in \*MAT\_SAMP-1 and Figure 9 shows the LS-DYNA result calculated with an adequately tuned damage property that fits the test result well.

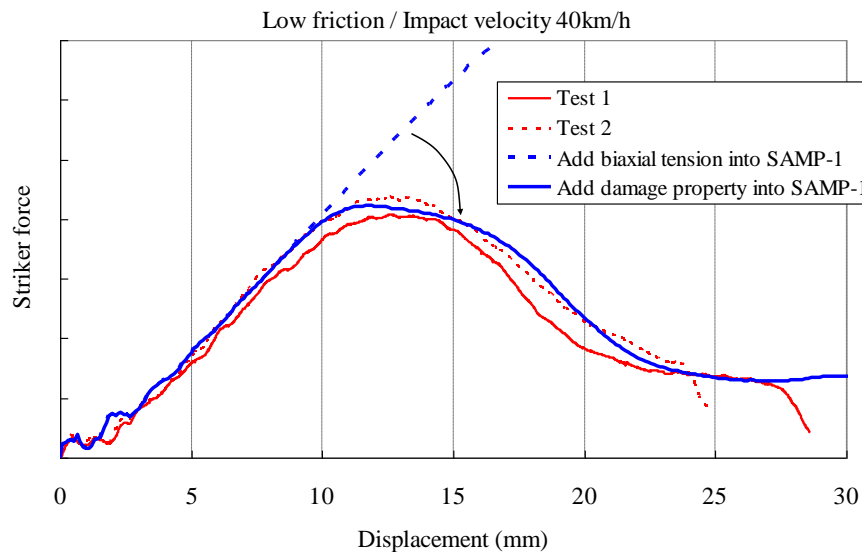


Figure 9: Striker force vs. displacement result with tuned damage property

Next, the modeling technology to predict rupture was investigated. Figure 10 shows the plastic strain distribution at the same time rupture was observed in test. The plastic strain was very large at over 300%. This predicted plastic strain is unlikely to be very accurate, considering the geometry and stability of such greatly stretched mesh, but it is undoubtable that the failure plastic strain under biaxial tension is much larger than the 15% to 60% seen under uniaxial tension. In order to predict this phenomenon, the LCSDG function of the GISSMO damage model in \*MAT\_ADD\_EROSION [8] was used. The LCSDG function calculates failure plastic strains based on stress triaxiality, which is determined by the deformation mode.

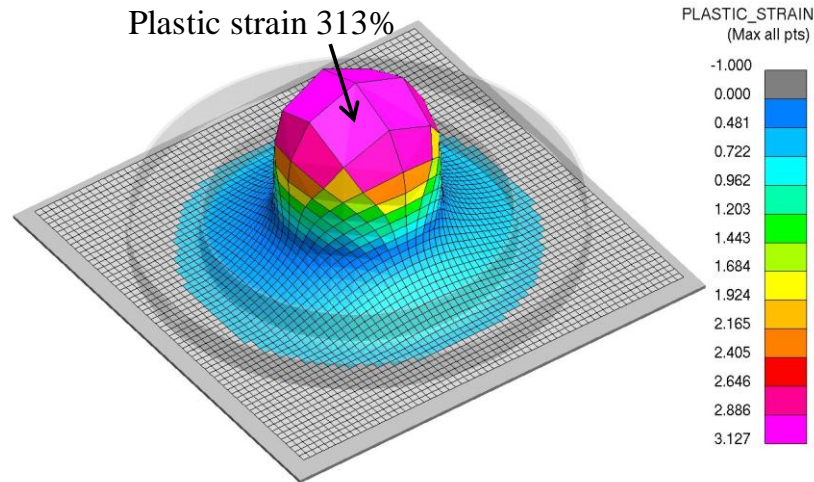


Figure 10: Plastic strain distribution at time of observed rupture

Figure 11 shows the failure plastic strain vs. stress triaxiality curve used in LCSDG. Biaxial tension (triaxiality 2/3) was given a failure plastic strain of 320% and uniaxial tension (triaxiality 1/3) was given 40% (an average of the 15% and 60% measured in test). Shear (triaxiality 0) was given the same 40% as uniaxial and compression (less than 0) was given an extremely large value so as to not to reach any failure state.

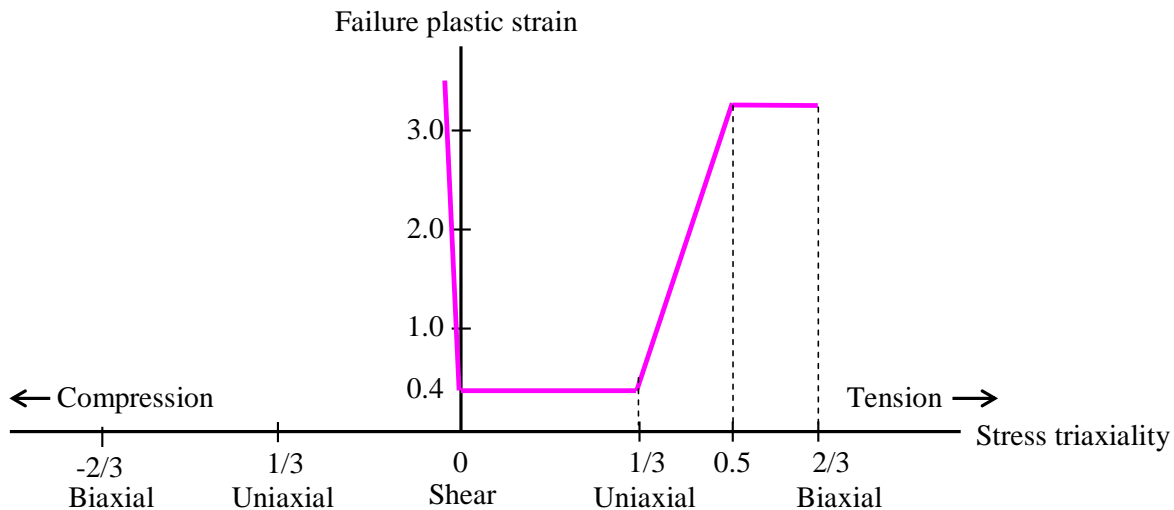


Figure 11: Failure plastic strain vs. stress triaxiality



Figure 12 shows the LS-DYNA result. The predicted deformation mode and rupture timing match test very well. A low friction condition was simulated and Petaling failure mode well predicted.

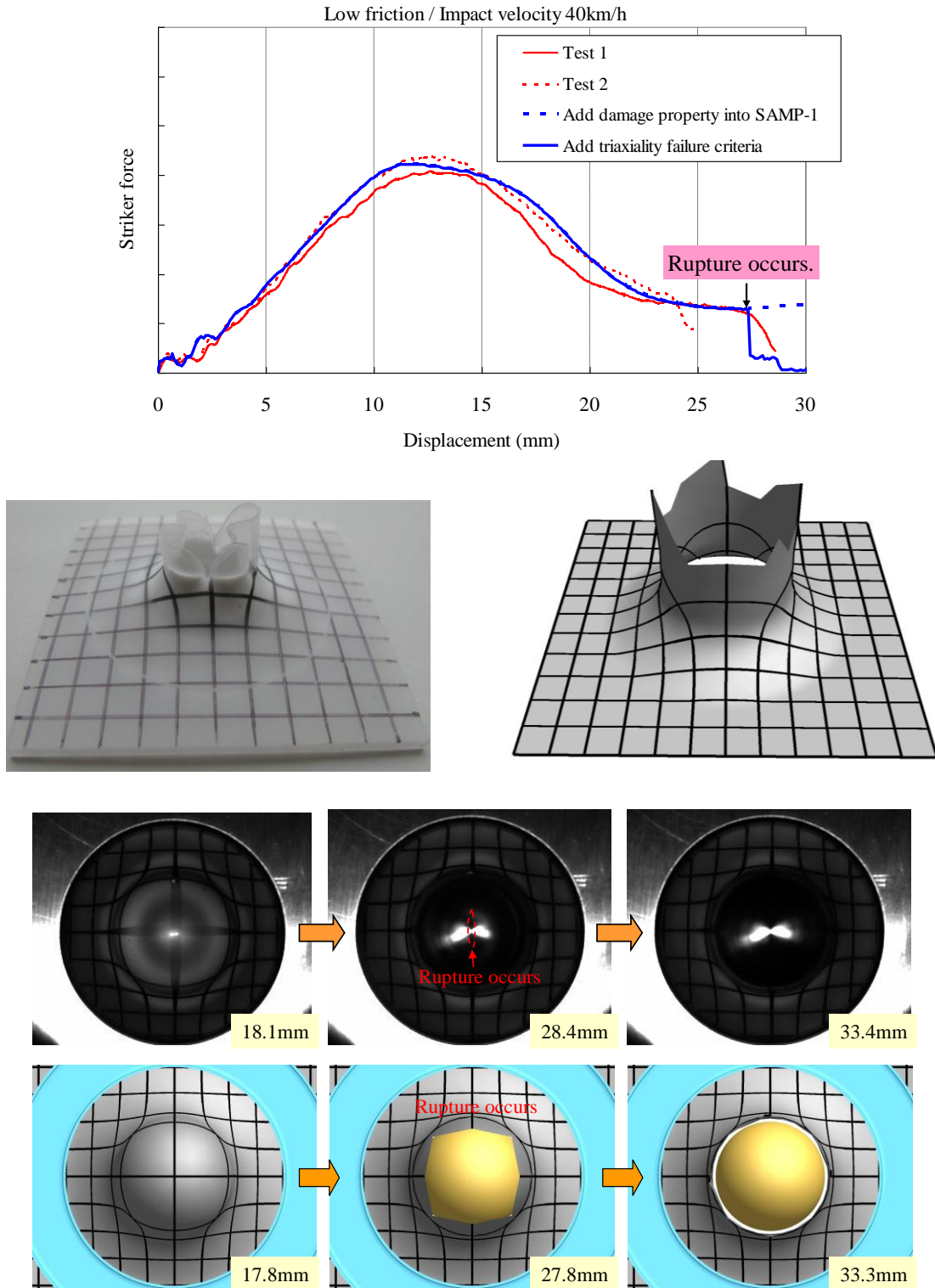


Figure 12: The final correlated LS-DYNA results of low friction and impact velocity 40km/h

### LS-DYNA Puncture test simulation under high friction

The high friction condition model was created by just setting the friction coefficient to 0.35 in the final correlated no friction model. Figure 13 shows that the high friction simulation predicted peak force as well as circumferential failure mode perfectly.

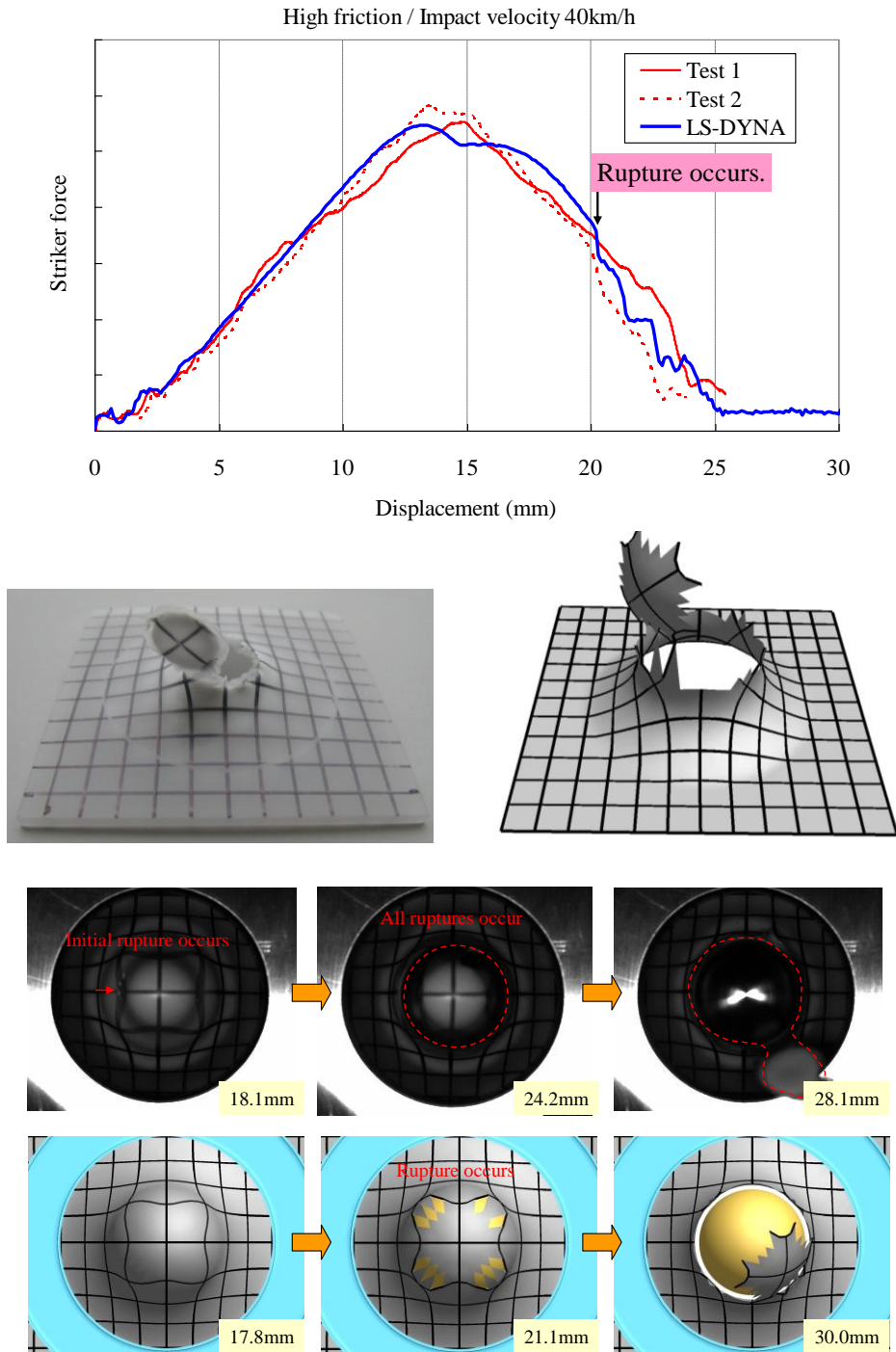


Figure 13: The final correlated LS-DYNA results of high friction and impact velocity 40km/h

The failure mechanism of the high friction case was briefly investigated. Figure 14 shows how the deformation of the sheet area in contact with the striker is restrained due to high friction. An area outside this under mainly uniaxial tension exists with higher plastic strain.

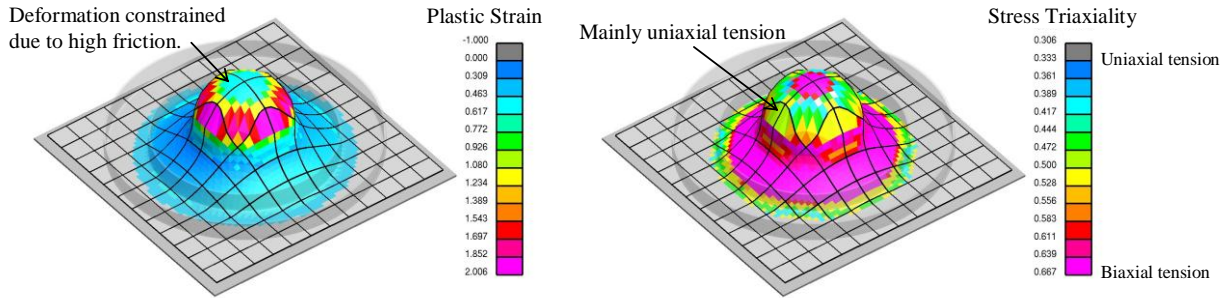


Figure 14: Plastic strain and stress triaxiality distributions of high friction case

Figure 15 shows developing levels of plastic strain vs. stress triaxiality in a shell element leading to a failure. In the low friction case, stress triaxiality of the shell element keeps at a constant 2/3 and plastic strain reaches the high biaxial failure criteria before becoming eliminated. In the high friction case, stress triaxiality of the shell element changes from biaxial tension to uniaxial tension and the shell is eliminated at the lower failure criterion. Different failure modes thus occur as a result of the different stress conditions under low and high friction.

$$\int \frac{d\varepsilon_p}{\varepsilon_f(\text{stress triaxiality})} \geq 1 \rightarrow \text{Element failure}$$

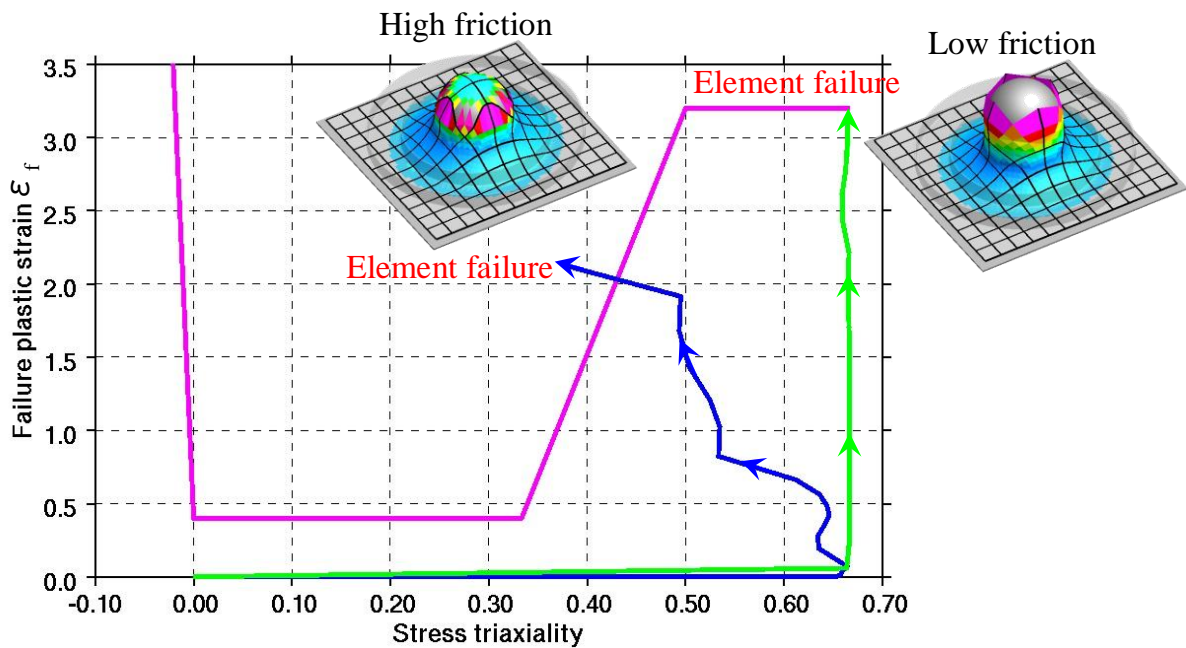


Figure 15: Plastic strain histories of a shell in low and high friction cases

## Investigation of new function for more accurate failure criteria

In the uniaxial tension test under quasi-static conditions (0.01/s), the polypropylene is very ductile. Therefore it is considered that the damage property of \*MAT\_SAMP-1 should have a new capability of strain rate and if possible, stress triaxiality dependency. Strain rate dependency of failure plastic strain vs. stress triaxiality is expected to be available by using the new damage initiation parameter P1 of \*MAT\_ADD\_EROSION. This is yet to be investigated. Figure 16 shows an example of strain rate dependent failure plastic strain vs. stress triaxiality.

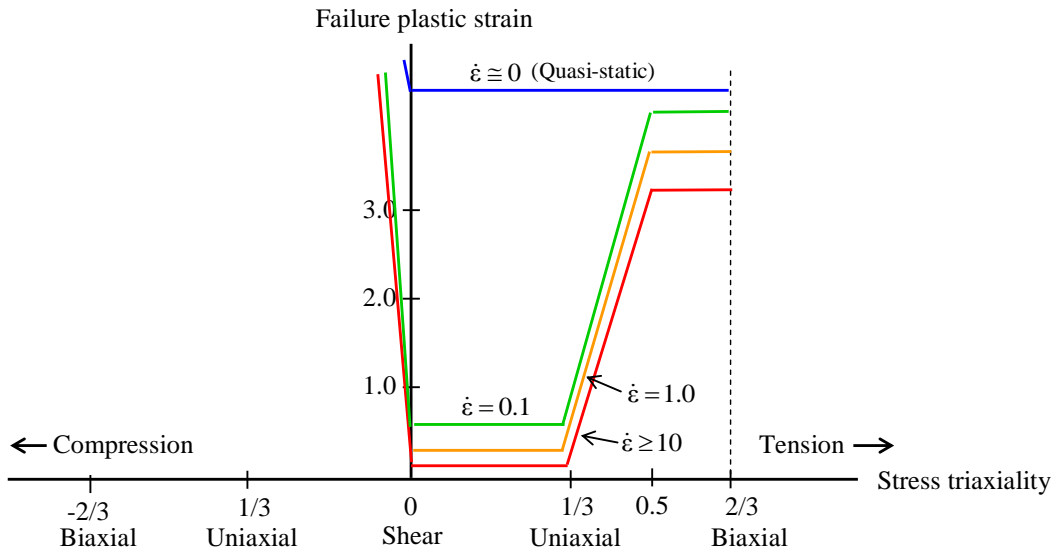


Figure 16: Example of strain rate dependency for failure plastic strain vs. stress triaxiality

## Conclusions

A material model to predict deformations and failures for a type of polypropylene has been successfully created using \*MAT\_SAMP-1 and \*MAT\_ADD\_EROSION. The following investigations are planned for future studies:

- 1) Puncture test simulations at different impact velocities will be performed and compared with test results.
- 2) Material tests under dynamic loading with special specimens generating stress triaxiality between 1/3 and 2/3 will be conducted in order to confirm failure criteria of failure plastic strain vs. stress triaxiality. Plans are also being made to measure failure plastic strain in shear deformation under high strain rates.
- 3) Puncture tests and simulations for other polymer materials will be performed.
- 4) Crash tests and simulations of components with more complicated geometry will be executed to validate this failure modeling.

## References

- [1] S. Kolling, A. Haufe, M. Feucht, P.A. Du Bois: SAMP-1: A Semi-Analytical Model for the Simulation of Polymers, LS-DYNA Anwenderforum, Bamberg, 2005

- [2] T. Glomsaker, E. Andreassen, M. Polanco-Loria, O.V. Lyngstad, R.H. Gaarder, E.L. Hinrichsen: Mechanical response of injection-moulded parts at high strain rates, PPS Europe/Africa Regional Meeting, Gothenburg, 2007
- [3] H. Mae, K. Kishimoto: Modeling and Simulation of Impact Failure Characteristic of Polypropylene by Elastoviscoplastic Constitutive Law, Journal of Solid Mechanics and Materials Engineering, 2007
- [4] G. Oberhofer, A. Bach, M. Franzen, H. Gese, H. Lanzerath: A Systematic Approach to Model Metals, Compact Polymers and Structural Foams in Crash Simulations with a Modular User Material, 7<sup>th</sup> European LS-DYNA Conference, Salzburg, 2009
- [5] H. Daiyan, F. Grytten, E. Andreassen, H. Osnes, R.H. Gaarder, E.L. Hinrichsen: Numerical simulation of low-velocity impact loading of polymeric materials, 7<sup>th</sup> European LS-DYNA Conference, Salzburg, 2009
- [6] R.Balieu, F.Lauro, B.Bennani, B.Bourel, K.Nakaya, E.Haran: Behaviour model for semi-crystalline polymer, application to crashworthiness simulations, 8<sup>th</sup> European LS-DYNA Conference, Strasbourg, 2011
- [7] LSTC: LS-DYNA KEYWORD USER'S MANUAL, February 2012 Version 971 R6.0.0
- [8] A. Haufe, M. Feucht, F. Neukamm, P.A. DuBois: Recent Enhancements to the GISSMO Failure Model in LS-DYNA, 8<sup>th</sup> European LS-DYNA Conference, Strasbourg, 2011
- [9] ISO 6603-2, 2000, Plastics-Determination of puncture impact behaviour of rigid plastics
- [10] H. Daiyan, E. Andreassen, F. Grytten, O.V. Lyngstad, T. Luksepp, H. Osnes: Low-velocity impact response of injection-moulded polypropylene plates – Part 1; Effects of plate thickness, impact velocity and temperature, Polymer Testing 29, 2010

